J|A|C|S
ARTICLES
Published on Web 08/30/2006

Microfluidic Production of Biopolymer Microcapsules with Controlled Morphology

Hong Zhang,[†] Ethan Tumarkin,[†] Raheem Peerani,[†,‡] Zhihong Nie,[†] Ruby May A. Sullan,[†] Gilbert C. Walker,[†] and Eugenia Kumacheva*[,†,‡,§]

Contribution from the Department of Chemistry, University of Toronto, 80 Saint George Street, Toronto, Ontario M5S 3H6, Canada, Institute of Biomaterials and Biomedical Engineering, Department of Materials Science and Engineering, University of Toronto, 4 Taddle Creek Road, Toronto, Ontario M5S 3G9, Canada, and Department of Chemical Engineering and Applied Chemistry, University of Toronto, 200 College Street, Toronto, Ontario M5S 3E5, Canada

Received May 22, 2006; E-mail: ekumache@chem.utoronto.ca

Abstract: We report a microfluidic approach to generating capsules of biopolymer hydrogels. Droplets of an aqueous solution of a biopolymer were emulsified in an organic phase comprising a cross-linking agent. Polymer gelation was achieved in situ (on a microfluidic chip) by diffusion-controlled ionic cross-linking of the biopolymer, following the transfer of the cross-linking agent from the continuous phase to the droplets. Gelation was quenched by collecting particles in a large pool of cross-linking agent-free liquid. The structure of microgels (from capsules to gradient microgels to particles with a uniform structure) was controlled by varying the time of residence of droplets on the microfluidic chip and the concentration of the cross-linking agent in the continuous phase. We demonstrated the encapsulation of a controlled number of polystyrene beads in the microgel capsules. The described approach was applied to the preparation of capsules of several polysaccharides such as alginate, κ-carrageenan, and carboxymethylcellulose.

Introduction

A microcapsule is a particle or a droplet with a well-defined shell and a solid, liquid, or gaseous core.[1] Microcapsules with hydrogel shells that are formed by biopolymers are used for the encapsulation and controlled release of drugs,[2] cosmetics,[3] pesticides,[4] and food additives.[5] Capsules of biopolymers show promising applications in the encapsulation of transplanted cells: a membrane protects the cells from rejection by the immune system and allows transplantation without the need for immunosuppression,[6] while a liquid core provides the cells with a microenvironment that ensures their unrestricted growth.[7]

Existing strategies for the preparation of polymer capsules include engulfment of templates (particles, droplets or bubbles) by a polymer shell,[8] generation of core−shell droplets followed by solidification of droplet shells,[9] and interfacial condensation reactions.[10] These methods involve multistage processes, employ materials that are not biocompatible, and do not allow precise control over dimensions, structure, and properties of the resulting capsules. Reproducible single-step production of monodisperse capsules of gelling biopolymers with control over capsular size, internal structure, and mechanical properties is in great demand.[11]

Recently, microfluidic methods have provided a facile approach to synthesis and fabrication of monodisperse polymer capsules in the micrometer size range.[12−14] Capsules were obtained by generating single or double emulsions followed by interfacial polycondensation[12] or solidification of droplet shells by means of photopolymerization[13] or by removal of the solvent from droplet shells.[14] Synthesis and fabrication of capsules of biopolymers have not yet been demonstrated.

[†] Department of Chemistry.
[‡] Institute of Biomaterials and Biomedical Engineering, Department of Materials Science and Engineering.
[§] Department of Chemical Engineering and Applied Chemistry.

(1) Mathiowitz, E. *Encyclopedia of Controlled Drug Delivery*; John Wiley & Sons: 1999; Vols. 1 and 2.
(2) Muraoka, M.; Hu, Z. P.; Shimokawa, T.; Sekino, S.; Kurogoshi, R.; Kuboi, Y.; Yoshikawa, Y.; Takada, K. *J. Controlled Release* **1998**, *52*, 119−129.
(3) Gebelein, C. G.; Cheng, T. C.; Yang, V. C. *Cosmetic and Pharmaceutical Applications of Polymers*; Plenum: New York, 1991.
(4) Blackmer, G. L.; Reynolds, R. H. *J. Agric. Food Chem.* **1977**, *25*, 559−561.
(5) El-Nakaly, M.; Piatt, D. M.; Charpentier, B. A. *Polymeric Delivery Systems, Properties and Applications*; American Chemical Society: Washington, D.C., 1993.
(6) (a) Sandberg, P. R.; Borlongan, C. V.; Othberg, A. I.; Saporta, S.; Freeman, T. B.; Cameron, D. F. *Nature Med. (N. Y., NY, U. S.)* **1997**, *3*, 1129−1132. (b) Dove, A. *Nat. Biotechnol.* **2002**, *20*, 339−343.
(7) Breguet, V.; Gugerli, R.; Pernetti, M.; von Stockar, U.; Marison, I. W. *Langmuir* **2005**, *21*, 9764−9772.
(8) (a) Donath, E.; Sukhorukov, G. B.; Caruso, F.; Davis S. A.; Möhwald, H. *Angew. Chem., Int. Ed.* **1998**, *37*, 2201−2205. (b) Lu, G.; An, Z. H.; Tao, C.; Li, J. B. *Langmuir* **2004**, *20*, 8401−8403. (c) Shchukin, D. G.; Köhler, K.; Möhwald, H.; Sukhorukov, G. B. *Angew. Chem., Int. Ed.* **2005**, *44*, 3310−3314.
(9) (a) Cellesi, F.; Weber, W.; Fussenegger, M.; Hubbell, J, A.; Tirelli, N. *Biotechnol. Bioeng.* **2004**, *88*, 740−749. (b) Babensee, J. E.; Cornelius, R. M.; Brash, J. L.; Sefton, M. V. *Biomaterials* **1988**, *9*, 839−849. (c) Lapitsky, Y.; Eskuchen, W. J.; Kaler, E. W. *Langmuir* **2006**, *22*, 6375−6379.
(10) Torini, L.; Argillier, J. F.; Zydowicz, N. *Macromolecules* **2005**, *38*, 3225−3236.
(11) Orive, G.; Hernández, R. M.; Gascón, A. R.; Calafiore, R.; Chang, T. M. S.; De Vos, P.; Hortelano, G.; Hunkeller, D.; Lacík, I.; Shapiro, A. M. J.; Pedraz, J. L. *Nat. Med.* **2003**, *9*, 104−107.
(12) (a) Takeuchi, S.; Garstecki, P.; Weibel, D. B.; Whitesides, G. M. *Adv. Mater.* **2005**, *17*, 1067−1072. (b) Quevedo, E.; Steinbacher, J.; McQuade, D. T. *J. Am. Chem. Soc.* **2005**, *127*, 10498−10499.
(13) (a) Loscertales, I. G.; Barrero, A.; Guerrero, I.; Cortijo, R.; Marquez, M.; Gañán-Calvo, A. M. *Science* **2002**, *295*, 1695−1698. (b) Nie, Z. H.; Xu, S. Q.; Seo, M. S.; Lewis, P. C.; Kumacheva, E. *J. Am. Chem. Soc.* **2005**, *127*, 8058−8063. (c) Oh, H. J.; Kim, S. H.; Baek, J. Y.; Seong, G. H.; Lee, S. H. *J. Micromech. Microeng.* **2006**, *16*, 285−291.

Microfluidic emulsification of gelled polymers is a challenge due to their high viscosity. Two existing microfluidic routes to biomicrogels employed postemulsification gelation. One approach involved formation of droplets of aqueous agarose solution at temperatures exceeding the gelation point of the polymer which, upon cooling, formed gel beads.[15] The need to control the temperature gradient across the microfluidic chip and the use of elevated temperatures limit the application of this method for fast throughput encapsulation of bioactive species. In the second approach in situ coalescence of droplets of an aqueous alginate solution and droplets of a cross-linking agent resulted in ionic cross-linking of the polymer and yields alginate particles.[16] The productivity of this method was limited by the probability of collisions of the droplets. Both approaches led to microgel beads with a uniform (noncapsular) structure.

The purpose of this study was to develop a microfluidic approach to generating capsules of *bio*hydrogels at room temperature, a 100% yield, and with good control of particle size distribution and internal structure. We produced capsules by emulsifying an aqueous solution of a biopolymer in an organic phase containing a dissolved cross-linking agent. This cross-linking agent had also a finite solubility in the water phase. Gelation of the droplets was achieved in situ (on a chip) by diffusion-controlled ionic cross-linking of the biopolymer, following the transfer of the cross-linking agent from the continuous phase to the drops. At the exit from the microfluidic device, gelation of the biopolymer was quenched by collecting particles in a large pool of the liquid that was free of the cross-linking agent. The structure of microgels was tuned by controlling the extent of gelation achieved on the chip, that is, by varying the time of residence of droplets on the chip and the concentration of cross-linking agent in the continuous phase.

We obtained capsules of several polysaccharides such as alginate, κ-carrageenan, and carboxymethylcellulose, with a particular focus on alginate capsules. Alginate beads have vast applications in the encapsulation of cells, proteins, and enzymes.[17] Generally, alginate microgels are prepared by external or internal diffusion of a cross-linking agent to or in the droplets of an aqueous alginate solution.[18] These methods yield large alginate beads with diameters in the range from 100 μm to several millimeters, polydispersities up to 20%, and poor control over the internal structure of particles.[19] In our work we obtained polysaccharide microgels in the size range from 30 to 200 μm, polydispersities below 4.0%, and precise control of the internal structure spanning from homogeneous microgels to capsules with the thickness of walls as small as several micrometers. Smaller and larger microgel beads can be produced by the same approach with an appropriate adjustment of the geometry of the microfluidic device.

Experimental Section

Materials. Sodium alginate (M_w = 240 000 g/mol), carboxymethylcellulose (M_w = 250 000 g/mol), fluo-3 ammonium salts, calcium chloride, calcium iodide, iron(III) nitrate nonahydrate, sorbitan monooleate (Span 80), and 1-undecanol were purchased from Aldrich Canada. κ-Carrageenan (M_w = 1 000 000 g/mol) was obtained from Copenhagen Hercules, Germany. Aqueous alginate solutions were dialyzed against deionized water at pH = 2 for 5 days to remove the traces of Ca^{2+} ions. The deionized water was obtained from the Millipore Milli-Q water purification system. Fluorescent polystyrene beads with the diameter 9.9 μm were supplied by Duke Scientific Corp., U.S.A.. SU-8 photoresist was purchased from MicroChem, U.S.A.. Sylgard 184 Silicon Elastomer kit was received from Dow Corning Corp. (Midland, MI).

Fabrication of Microfluidic Reactors. Masters were prepared with an SU-8 photoresist in bas-relief on silicon wafers. The microfluidic device was fabricated in poly(dimethylsiloxane) (PDMS) by using a standard soft-lithography method.[20]

Emulsification of Aqueous Solutions of Biopolymers. Two immiscible liquids, an aqueous solution of a biopolymer, and an undecanol solution of the cross-linking agent were supplied to the microchannels using two digitally controlled syringe pumps (Harvard Apparatus PHD 2000, U.S.A.). For the production of alginate and κ-carrageenan microgels, we used a solution of CaI_2 in undecanol. Carboxymethylcellulose microgels were obtained by using a solution of $Fe(NO_3)_3$ in undecanol. An Olympus BX51 microscope and a high-speed digital camera (Photometrics CoolSNAP ES) were used to acquire images.

Characterization of Microgels. Distribution of sizes of microgels and the corresponding droplets were characterized by analyzing optical microscopy images of 250 particles or droplets using Image Pro (Media Cybernetics) software.

Viscosities of the aqueous solution and gels of alginate were measured using a Brookfield rheometer (Brookfield, U.S.A.).The distribution of Ca^{2+} ions in the microgel capsules was characterized using scanning confocal microscopy (Leica TCS SP2) with a 20× dry objective, NA = 0.5 at $\lambda_{ex} = 488 \pm 20$ nm and $\lambda_{em} = 525 \pm 25$ nm. The concentration of ions in the microgels was determined by using Inductively Coupled Plasma-Atomic Emission Spectroscopy (ICP-AES) (Optima 3000) instrumentation. Prior to measurements, the biomicrogels were digested in a H_2SO_4/HNO_3 (8:3 v/v) mixture at 60 °C and diluted by the deionized water (the volume ratio of H_2SO_4/H_2O was 8:39). Mechanical properties of the microgels were characterized by indentation measurements using an atomic force microscope (Digital Instruments Dimension 5000, Santa Barbara, CA). A silicon nitride probe (DNP, Veeco) with a force constant of $\sim$0.6 N m^{-1} was applied in the force mode. After indenting the surface of the microgel, the probe was lifted off the sample surface. An optical lever detection system was used to measure the deflection of the probe tip. A force curve was obtained by plotting the deflection of the AFM tip as a function of the vertical displacement of the piezo scanner. Using the software provided by Digital Instruments, we collected the force curves and converted them into the force versus indentation graphs. Indentations were limited to tens of nanometers. Custom software written in MATLAB (Natick, MA) was used to extract the elastic modulus of the microgels. The elastic moduli of the microgels were determined by assuming a conical tip shape[21] which produced a load-indentation dependence as follows

$$F = \frac{2E \tan \alpha}{\pi(1 - \upsilon^2)} \delta^2 \quad (1)$$

where F is the loading force in newtons, δ is the indentation in meters, E is Young's modulus in pascals, υ is the Poisson's ratio (0.5), and α is the tip semivertical angle (35°). The intercept of the log−log graph of F versus δ (eq 2) gave the Young's modulus of the microgels

(14) Utada, A. S.; Lorenceau, E.; Link, D. R.; Kaplan, P. D.; Stone, H. A.; Weitz, D. A. *Science* **2005**, *305*, 537−541.
(15) Xu, S. Q.; Nie, Z. H.; Seo, M.; Lewis, P.; Kumacheva, E.; Stone, H. A.; Garstecki, P.; Weibel, D. B.; Gitlin, I.; Whitesides, G. M. *Angew. Chem., Int. Ed.* **2005**, *44*, 724−728.
(16) Sugiura, S.; Oda, T.; Izumida, Y.; Aoyagi, Y.; Satake, M.; Ochiai, A.; Ohkohchi, N.; Nakajima, M. *Biomaterials* **2005**, *26*, 3327−3331.
(17) (a) Seifert, D. B.; Phillips, J. *Biotechnol. Prog.* **1997**, *13*, 562−568. (b) Gombotz, W. R.; Wee, S. F. *Adv. Drug Delivery Rev.* **1998**, *31*, 267−285.
(18) Sanderson, G. R.; Ortega, D. Alginates and gellan gum: complementary gelling agents. In *Food Hydrocolloids: Structure, Properties, and Functions;* Nishinari, K., Doi, E., Eds.; Plenum Press: New York, 1993.
(19) Yang, F.; Wang, K.; He, Z. M. *Int. J. Pharm.* **2005**, *298*, 206−210.
(20) Xia, Y. N.; Whitesides, G. M. *Angew. Chem., Int. Ed.* **1998**, *37*, 550−575.
(21) Sneddon, I. N. *Int. J. Eng. Sci.* **1965**, *3*, 47−57.

$$\log F = \log\left[\frac{2E \tan \alpha}{\pi(1 - \upsilon^2)}\right] + 2 \log \delta \qquad (2)$$

Results and Discussion

Diffusion-Controlled Gelation of Bulk Phases. Prior to microfluidic experiments, we examined time-dependent and concentration-dependent gelation of biopolymers, governed by diffusion of the cross-linking agent from an organic to an aqueous phase. Figure 1a shows photographs of an aqueous solution of alginate brought in contact with a solution of CaI_2 in undecanol for various time intervals. The solubilities of CaI_2 in undecanol and water are 16.4 g/L and 2.150×10^3 g/L, respectively.[22−24] Following diffusion from undecanol to the aqueous phase, Ca^{2+} ions bound to the residues of α-L-guluronic (G) acid of alginate causing polymer gelation.[18] The extent of gelation of alginate depended on the time that the macroscopic phases were kept in contact. In Figure 1a, a 2 min gelation period produced a thin (ca. 1 mm thick) layer of a gel, while a 4 min period resulted in complete gelation of the alginate solution (Figure 1a).With increased concentration of CaI_2 in undecanol, the time required for gelation of alginate decreased.

Microfluidic Emulsification of Biopolymer Solution. Figure 1b shows formation of droplets of alginate solution in the planar microfluidic device with a Y-shaped orifice. An aqueous alginate solution with a typical viscosity from 34.2 to 64.0 cP and an undecanol solution of CaI_2 were forced into the orifice where a thread of alginate solution periodically broke up to release droplets. Formation of droplets occurred in the flow-focusing regime.[25] The downstream channel was followed by the wavy microchannel (Figure 1c) in which diffusion of Ca^{2+} ions from undecanol to the droplets caused gelation of alginate. Undecanol was selected as a continuous phase for several reasons: (i) undecanol does not swell PDMS and therefore does not alter the dimensions of microchannels in the course of experiments; (ii) undecanol dissolves 16.4 g/L of CaI_2 and has an insignificant solubility in water of 20.5 ppm;[26] (iii) alginate microgels can be easily transferred from undecanol to an aqueous phase; (iv) undecanol has a higher viscosity of 11.8 cP[26] compared to lower alcohols, and thus it favors stable formation of aqueous droplets with a narrow size distribution (higher alcohols are solid at room temperature).

The diameter of alginate droplets decreased with increasing flow rate of undecanol, Q_o, or decreasing flow rate of alginate solution, Q_w (Figure 1d, solid lines). Droplets with a narrow size distribution formed for $8.0 < Q_o/Q_w < 18$; outside this range of flow rate ratios of liquids the main population of droplets was accompanied by small satellite droplets. By changing the values of Q_o from 0.2 to 15 mL/h and Q_w from 0.30 to 0.70 mL/h we obtained alginate droplets with diameters from 30 to 230 μm and polydispersities of 2.2 ± 0.2%.

For comparison, Figure 1e shows a thread of 0.50 wt % alginate solution premixed with 0.10% solution of $CaCl_2$ and flow-focused by the shear stress imposed by mineral oil (a continuous phase) in a five-channel microfluidic device.[13b] Although the concentrations of the polymer and $CaCl_2$ were lower than those in the previous experiment, mixing of aqueous solutions of alginate and the cross-linking agent instantaneously increased the viscosity of the resulting system to 1440 cP (measured at a shear rate of 46.0 s^{-1}). The resulting thread formed nodules but did not break up in droplets in a wide range of flow rates of the continuous phase.

Diffusion-Controlled Gelation in Microfluidic Devices. Aqueous droplets of biopolymers obtained in the downstream channel moved to the wavy channel where diffusion of CaI_2 from the continuous phase to the droplets led to polymer gelation. We observed the first indication of gelation as the appearance of small islands of a "skin" on the surface of droplets (Figure 2a). In the control experiment, "skinning" was not observed when alginate droplets were exposed to undecanol free of the cross-linking agent. With increasing time of residence of droplets in the wavy channel, the entire surface of droplets gradually acquired a characteristic grain structure. The time interval between the formation of droplets and the first sign of "skinning" (typically, between 33 and 61 s) depended on the concentration of CaI_2 in undecanol, consistent with our observations of diffusion-controlled gelation of bulk phases of alginate solution (Figure 1a).

The particles emerging from the wavy channel were collected in 50 mL of undecanol free of cross-linking agent. Figure 2b,d,e shows typical optical microscopy images of microgels of alginate, κ-carrageenan, and carboxymethylcellulose, respectively. The latter polymer was cross-linked by Fe^{3+} ions. Typically, the mean diameter of microgels was 8−10% smaller than that of the corresponding droplets, as shown for alginate microgels in Figure 1d (dotted lines). Figure 2c shows alginate microgels transferred to a PBS solution (pH = 7.4) by centrifuging the microgel dispersion in undecanol at 1500 *g*, removing the supernatant, and washing the capsules with a PBS buffer. In the PBS solution the particles retained their stability and narrow size distribution, as shown in Figure 2f. A slightly larger size of alginate microgels in the buffer versus undecanol was due to excess osmotic pressure in the interior of the microcapsules. The productivity of the single microfluidic device was up to 5000 particles/min.

Morphology of Microgels. Based on the results shown in Figure 1a, the thickness of a gelled layer in the droplets depended on the time of diffusion of CaI_2 in the aqueous phase (controlled by the time of residence of the droplets on the chip) and the concentration of CaI_2 in undecanol. The time of diffusion is determined by the velocity of droplets and the length of the wavy channel (shown in Figure 1c). We examined the distribution of Ca^{2+} ions in the microcapsules by emulsifying an alginate solution premixed with 0.01 mM dye fluo-3 and examining the structure of microgels using confocal fluorescence microscopy. In the presence of Ca^{2+} ions, fluo-3 gains photoluminescence,[27] and thus it can be used as a tracer of calcium ions in the microgel particles.

Figure 3 shows typical confocal fluorescence microscopy images of alginate microgels. With increasing concentration of CaI_2 in undecanol solution (Figure 3a−d) and increasing time

(22) Data obtained in ICP-AES measurements.
(23) Lide, D. R. *Handbook of Chemistry and Physics*, 83th ed.; CRC Press: 2002−2003.
(24) Increase in conductivity of undecanol from 1.42 to 6.42 μS in the presence of 2.0 wt % CaI_2 suggests that in undecanol CaI^2 dissociates into Ca^{2+} and I^- ions.
(25) (a) Anna, S. L.; Bontoux, N.; Stone, H. A. *App. Phys. Lett.* **2003**, *82*, 364−366. (b) Garstecki, P.; Stone, H. A.; Whitesides, G. M. *Phys. Rev. Lett.* **2005**, *94*, 164501−4.
(26) Yaws, C. L. *Chemical Properties Handbook*; MaGraw-Hill: 1999.
(27) (a) Hagar, A. F.; Spitzer, J. A. *Cell Calcium* **1992**, *13*, 123−130. (b) The data are obtained from the website of Molecular Probes (www.invitrogen-.com) U.S.A.

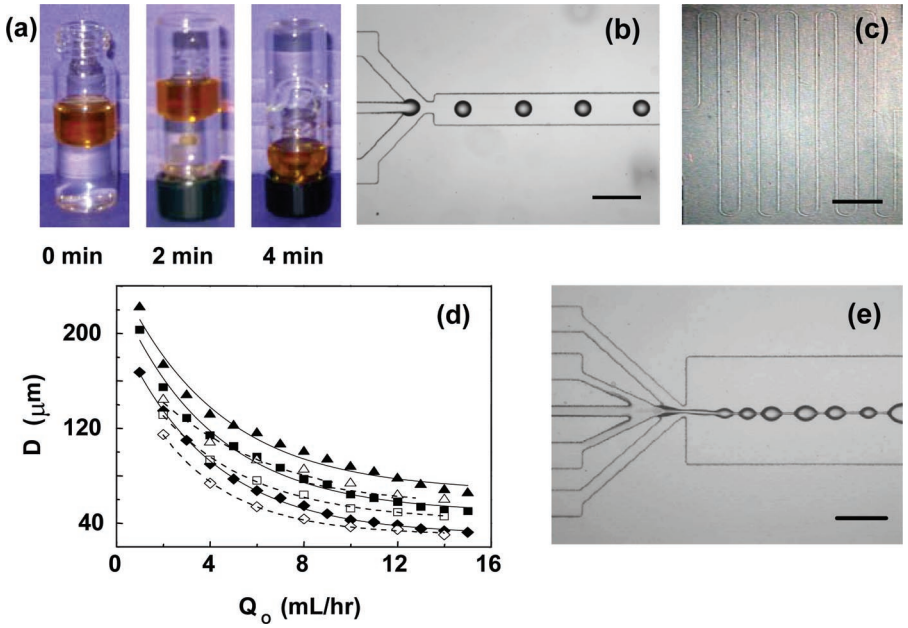

Figure 1. (a) Time-dependent gelation of alginate driven by diffusion of Ca^{2+} ions from undecanol to an aqueous solution of alginate. Photographs from left to right show vials with an aqueous 0.50 wt % alginate solution brought in contact with 2.0 wt % CaI_2 solution in undecanol for 0, 2, and 4 min. (b) Optical microscopy image of droplets of 1.0 wt % alginate solution emulsified in a Y-shaped microfluidic device in 0.2 wt % undecanol solution of CaI_2. Orifice height and width are 130 and 110 μm, respectively. Scale bar is 300 μm. (c) Optical microscopy image of the extension wavy channel with length 244 mm and width 350 μm. Scale bar is 3 mm. (d) Variation in mean diameter of alginate droplets (filled symbols) and corresponding microgel capsules (open symbols) as a function of flow rate, Q_o, of undecanol solution for Q_w = 0.30 mL/h (◆,◇), 0.50 mL/h (■, □), 0.70 mL/h (▲, △). Droplets with diameter exceeding the height of the microchannel of 130 μm acquired a discoid shape. The concentrations of alginate and CaI_2 in undecanol were 2.0 and 0.50 wt %, respectively. (e) Formation of nodes on the liquid thread of 0.50 wt % aqueous alginate solution mixed with 0.10 wt % of $CaCl_2$ in coflowing mineral oil in a five-channel microfluidic device. Alginate solution, solution of $CaCl_2$, and mineral oil were introduced in the central, intermediate, and outer channels, respectively, at flow rates 0.2, 0.05, and 10 mL/h, respectively. Scale bar is 300 μm.

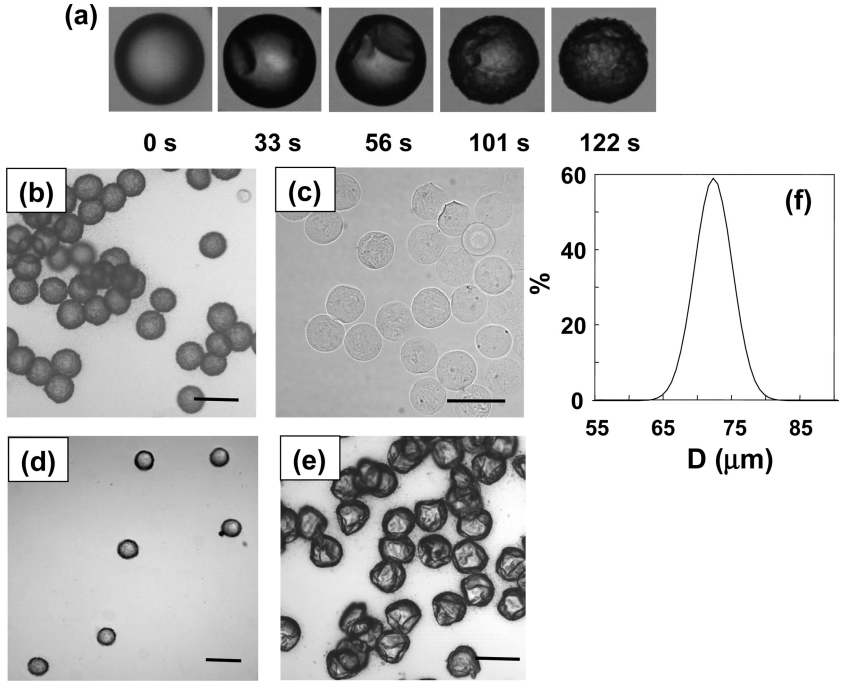

Figure 2. (a) Optical microscopy images (top view) of alginate droplets in the wavy channel exposed for different time intervals to 0.15 wt % undecanol solution of CaI_2. (b) Micrograph of alginate microgels obtained by emulsifying 1.0 wt % alginate solution in 0.20 wt % undecanol solution of CaI_2. Q_w = 0.03 mL/h, Q_o = 0.20 mL/h. (c) Micrograph of alginate microgels transferred to a PBS solution at pH 7.4. (d) Micrograph of κ-carrageenan microgels obtained by emulsifying 0.80 wt % solution of κ-carrageenan in a 0.25 wt % undecanol solution of CaI_2. Q_w = 0.03 mL/h, Q_o = 0.35 mL/h. (e) Micrograph of carboxymethylcellulose microgels obtained by emulsifying 1.0 wt % solution of carboxymethylcellulose in 0.25 wt % undecanol solution of $Fe(NO_3)_3$. Q_w = 0.03 mL/h, Q_o = 0.25 mL/h. The scale bar is 100 μm in (b−e). (f) Size distribution of alginate microgels. Polydispersity of microgels is 3.8%. The experimental points were fitted with a Gaussian distribution.

of gelation (Figure 3c, e, f), the thickness of Ca^{2+}-rich zones in the microgels increased until a uniform distribution of calcium in the particles was reached. The localization of Ca^{2+} ions in microgel shells was preserved after the 5-day storage of particles

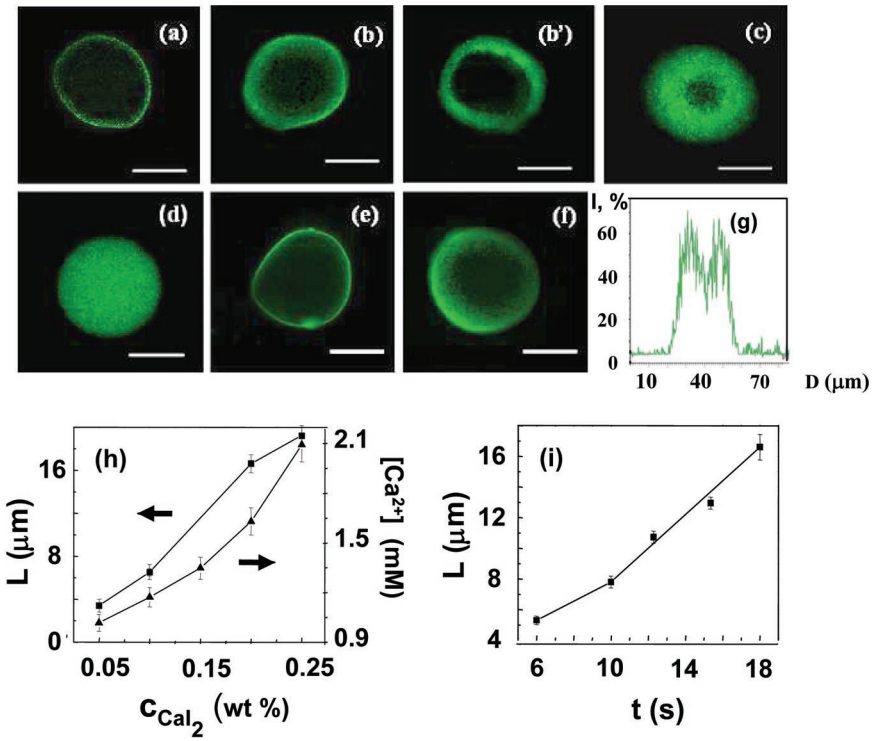

Figure 3. Confocal fluorescence microscopy images of alginate microgels obtained by emulsification of 1.0 wt % alginate solution in a solution of CaI_2 in undecanol with concentrations, wt %: (a) 0.05, (b, b′) 0.10, (c, e, f) 0.20, and (d) 0.25. In (b′) microgels were stored for 5 days in CaI_2-free undecanol. Gelation time was 18 s for (a−d) and 6 and 10 s for (e) and (f), respectively. (g) Representative profile of fluorescent density for the alginate microcapsule shown in (c). (h) Variation in depth of penetration of Ca^{2+} ions in microgels (■) and concentration of Ca^{2+} ions (▲) in microgels. (i) Depth of penetration of Ca^{2+} ions in microgels versus gelation time. Scale bar is 20 μm. In (h,i) the lines are added for visual guidance.

in pure undecanol (Figure 3b′). We plotted fluorescence line profiles, as in Figure 3g, and determined the thickness, L, of Ca^{2+}-rich shells. In Figure 3h variation in thickness of fluorescent shells versus the concentration of CaI_2 in the continuous phase and diffusion time showed an increase in thickness of Ca^{2+}-rich layers. Since the "sensitivity" of fluo-3 detecting Ca^{2+} ions is as small as 0.325 μM,[27b] we assumed that Ca^{2+} ions are mostly localized in the bright zones of the microgels (as in Figure 3a−f) and calculated the concentration of Ca^{2+} ions in the particle shells to be from 1.64 to 2.38 mM. Based on the results of the control experiments carried out for bulk alginate solutions, such a concentration of Ca^{+} ions is sufficient to induce gelation of alginate. Thus the change in a single variable (the concentration of the cross-linking agent in the coflowing organic phase or the time of gelation) allowed control over the morphology of alginate microgels.

Since the laminar flow of two immiscible liquids does not significantly change the diffusion of Ca^{2+} ions from undecanol to the droplet phase,[28] diffusion-controlled gelation of alginate could be approximated with eq 3 describing the diffusion accompanied by an instantaneous chemical reaction,[29] i.e., binding of Ca^{2+} ions to the carboxylic groups on alginate

$$\frac{\partial C}{\partial t} = D\frac{\partial^2 C}{\partial t^2} - \frac{\partial S}{\partial t} \qquad (3)$$

where D is the diffusion coefficient of Ca^{2+}, C is the concentration of Ca^{2+} ions in undecanol, and S is the concentration of

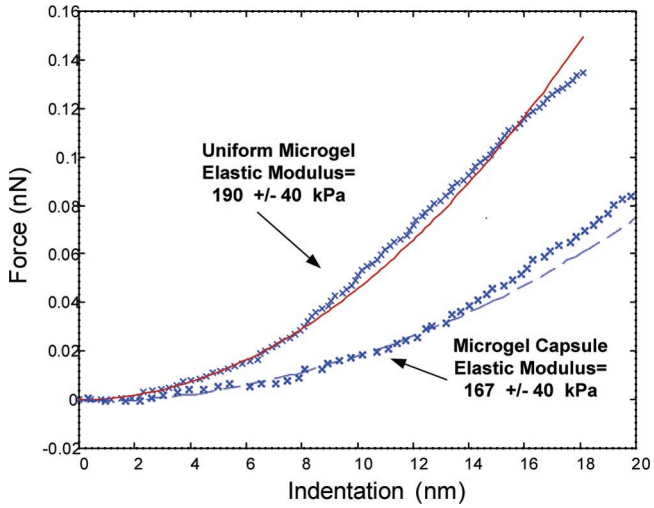

Figure 4. Force indentation curves of microgel capsules and microgels with a uniform internal structure. The solid and the broken lines represent the fit by the conical tip model (eq 1) to indentation data on the microgel with uniform morphology (upper curves) and the microcapsules (lower curves), respectively. The crosses are the data points. 190 and 167 kPa represent the average moduli obtained from many indentation profiles for the uniform microgel and the microgel capsule, respectively.

cross-linked Ca^{2+} ions. The penetration of Ca^{2+} ions in the microgels was governed by the concentration of Ca^{2+} ions in undecanol, time of diffusion, and kinetics of cross-linking. At low concentration of Ca^{2+} ions in undecanol and/or the short time of residence of microgels on the microfluidic chip, the second term in eq 3 dominated formation of the microcapsules. Microgels with a uniform structure formed when Ca^{2+} ions diffused to the center of the particles, that is, when the

(28) Squires, T. M.; Quake, S. R. *Rev. Mod. Phys.* **2005**, *77*, 977−1026.
(29) Crank, J. *The Mathematics of Diffusion*, 2nd ed.; Oxford: Clarendon Press: 1975.

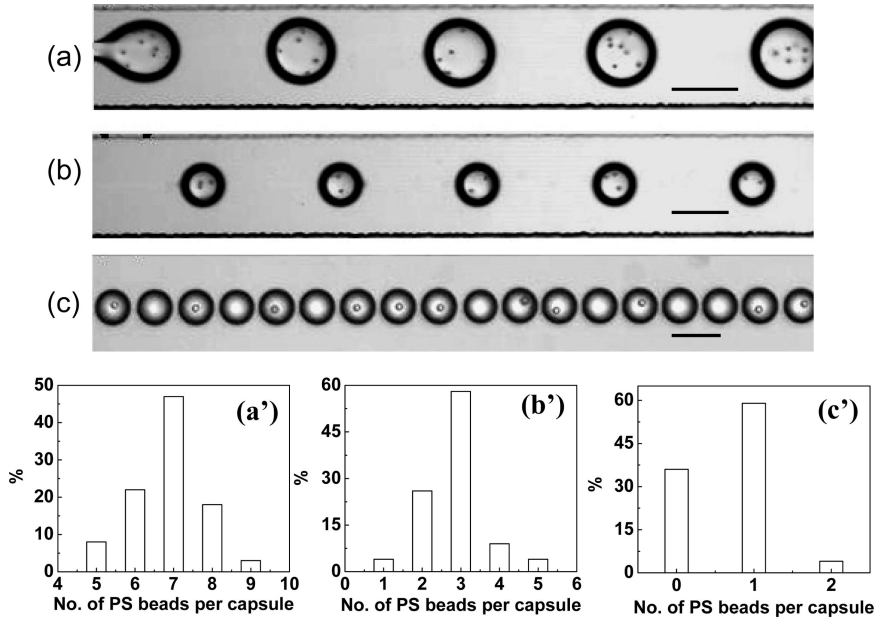

Figure 5. (a−c) Optical microscopy images of polystyrene (PS) beads encapsulated in alginate capsules with the average diameter 150 μm (a), 100 μm (b), and 30 μm (c). Scale bars are 150 μm (a, b) and 50 μm (c). (a′−c′): Histograms of distribution of the number of PS beads per individual alginate capsule, as shown in (a−c), respectively. Concentration of alginate was 1.0 wt %. Concentration of PS beads in aqueous alginate solution was 2×10^6 particles/mL. $Q_w = 0.05$, 0.08, and 0.10 mL/h and $Q_o = 0.5$, 0.8, and 1.2 mL/h for (a−c), respectively.

concentration of Ca^{2+} ions in undecanol was high or the time of residence of particles on the chip was sufficiently long.

Mechanical Properties of Microgels. We used atomic force microscopy (AFM) experiments to determine the elastic modulus of alginate capsules and microgels with a uniform morphology (Figure 4). The elastic modulus of microgels with a uniform structure was slightly higher than that of the capsules; however for both particles the values of elastic moduli were close to the values reported by Ouwerx et al.[30] for the alginate beads prepared by dropping a solution of sodium alginate in the solution containing Ca^{2+} ions. We note that indentation of the cantilever was only dozens of nanometers deep in the microgel and therefore did not detect the thickness of the gelled alginate layer of ca. 3.4 μm in microcapsules (Figure 3a).

Controlled Encapsulation of Polystyrene Beads. We explored the potential application of the described strategy for the encapsulation of a controlled number of cells per capsule. As a model system we used 9.9 μm diameter polystyrene (PS) beads. Figure 5 shows typical micrographs and histograms for the distribution of PS particles in alginate capsules. The average number of PS beads per droplet was controlled by varying the diameter of alginate particles. The average number of beads per capsule was 7 and 3 for the 150 μm and 100 μm size capsules, respectively. We also produced a large population of 30 μm size microgels containing a single PS particle (about 36% of capsules were particle-free). In comparison with a recent report of Tan et al.[31] on the variation in the number of particles encapsulated in lipid vesicles, our strategy provides an efficient control over the number of particles per microcapsule.

These results show that with an appropriate selection of reactants the described method may be useful for the direct encapsulation of individual cells or the encapsulation of cells with other active biological species such as enzymes, cytokines, and extracellular matrix. Precise control over the structure of microgels allows for different physical and mechanical microenvironments to be presented to cells. These different microenvironments may facilitate gas and nutrient exchange with the exterior media and provide a compliant surface for cell expansion.

In summary, we have reported a microfluidic route to fast throughput production of monodisperse capsules of biopolymers via emulsification of biopolymer solutions and diffusion-controlled gelation. By controlling the time of gelation and/or the concentration of the cross-linking agent in the continuous phase we achieved control over the internal structure of biomicrogels from capsules to gradient microgels to microgels with a uniform structure. Furthermore, for the model system we demonstrated the encapsulation of a controlled number of microbeads per capsule.

Acknowledgment. E.K. and G.W. acknowledge Canada Research Chair funding (NSERC Canada), G.W. acknowledges funding from ONR (N00014-05-0765), ARO (W911NF-04-1-0191) and NIH (R21-EB003101). H.Z. acknowledges the Martin Moskovits Ontario Graduate Scholarship in Science and Technology, and R.P. is grateful to the Ontario Graduate Scholarship Program. The authors thank Kyle Bishop, Siowling Soh, and Prof. Bartosz A. Grzybowski (Northwestern University) for assistance in analyzing diffusion-controlled gelation of biopolymers.

Supporting Information Available: Correlation of relative dissipated energy for alginate microgels versus cycle time of AFM tip. This material is available free of charge via the Internet at http://pubs.acs.org.

JA0635682

(30) Ouwerx, C.; Velings, N.; Mestdagh, M. M.; Axelos, M. A. V. *Polym. Gels Networks* **1998**, *6*, 393−408.
(31) Tan, Y. C.; Hettiarachchi, K.; Siu, M.; Pan, Y. R.; Lee, A. P. *J. Am. Chem. Soc.* **2006**, *128*, 5656−5658.